Computer-Aided Analysis of Conditions for Optimising Practical Electrorotation.

Michael Pycraft Hughes

Bioelectronics Research Centre,

University of Glasgow,

Glasgow, Scotland, G128QQ, UK

Tel: (+44) 141 330 5979

Fax: (+44) 141 330 4907

Email: pycraft@rank-serv.elec.gla.ac.uk

Short title: Analysis for Optimising Electrorotation

Keywords: Dielectrophoresis, AC Electrokinetics, cells, separation, electrodes, comparison

PACS: 02.70.Rw, 07.05.Pj, 87.22.-q, 87.80.+s

Abstract

Previous studies have indicated that the variations in torque induced in particles in Electrorotation electrode arrays are sufficiently large to cause errors in electrorotation measurements. In order to avoid this, experimenters usually study particles bound by an arbitrary region near the centre of the electrodes. By simulating the time-dependent electric field for polynomial electrodes, we have assessed the variation in torque across the centre of the array. By considering both the variation in applied torque and the dielectrophoretic force in the electrode chamber, the optimal conditions for electrorotation experiments have been determined. Further to this, by comparing the torque variation across the electrode chamber for a number of common electrode designs, a comparison of the suitability of each electrode design for multi-particle Electrorotation analysis has been made.

1. Introduction

Electrorotation (ROT) is a technique whereby particles suspended in rotating electric fields are caused to rotate (e.g. Arnold and Zimmermann 1982; Zhou *et al* 1995; Hölzel and Lamprecht 1992). The rate and direction of rotation are not synchronous with the rotating field, which may revolve at frequencies in excess of 1GHz (Hölzel 1997); rather, a torque is induced by the interaction between the rotating field and the dipole induced within the body. Since the properties of the induced dipole are frequency-dependent (Huang *et al* 1992), a measurement of ROT angular velocity as a function of applied frequency can be used to generate a "fingerprint" of the dielectric properties of the body. Such techniques have, for example, been used to monitor the infection cycle of Herpes Simplex in cells (Archer *et al* 1997), to identify the presence of bacteria adhered to the surface of rotating beads (Burt *et al* 1995), or determine the electrical properties of the various compartments of yeast cells (Huang and Pethig 1991).

When using ROT to determine the dielectric properties of bioparticles such as cells, it is often preferable to study the rotation behaviour of a population of cells distributed across an electrode chamber across which the electric field is applied using four electrodes in quadrature. It is a known fact that the electric field varies across the electrode chamber, as established by computer simulations (Gimsa *et al* 1987, Hölzel 1993, Hughes *et al* 1994) of the induced torque as a function of particle position within the chamber. This has obvious implications for the validity of ROT-derived data, particularly for particles whose position changes during the experiment.

Previous studies by Gimsa *et al* (1987) and Hölzel (1993) introduced correction factors for ROT work dependent on static field analysis (i.e. not considering phase effects), which have been widely used in the literature. However, as illustrated by Hughes *et al* (1994) it is important to consider the phase relationship between the electric field components which deviate from 90^{o} away from the centre of the electrode chamber.

Recent work by De Gasperis *et al* (1998) and Zhou *et al* (1998) have led to the inception of automated systems for determining ROT rates. Such a system can be adapted to adjust ROT data automatically. However, many researchers still perform ROT experiments manually, by counting the number of revolutions made by particles during a given time period. In this case, applying a position-determined correction factor is time-consuming and impractical.

For many years, it has been known that the torque varies widely, by observation of differing rotation rates across the chamber. In practice the experimenter selects which particles to study so as to ensure the results are meaningful. For example, Arnold and Zimmermann (1982) studied only those particles "within the central volume" , Zhou *et al* (1994), "within the central region between the electrode tips", and Chan *et al* (1997) restricted studies to those particles within a circle of radius defined by 1/3 of the distance from chamber centre to electrode tip. The dimensions of the limits set in these cases are arbitrary, having been decided upon by observation of the regions where the torque varies by only a small amount. Here we attempt to quantify this procedure by determining how the torque varies across the centre of the electrode chamber. Simulation methods have been used to determine the region of the electrode chamber within which the torque is approximately constant (for example, within +/-10%); the

dielectrophoretic forces which induce particle drift are also considered. This allows the researcher to determine which particles to observe in order to obtain a meaningful result.

Since the size and shape of this region will vary according to the geometry of the electrodes used, analyses of ten popular electrode designs are compared. By considering both the torque variation within this region (and hence the efficiency of the measurement technique) and the magnitude of torque generated, it is possible to make qualitative comparisons of the effectiveness of electrode efficiency.

2. Simulation Model

The simulation model was developed using Moments methods (Birtles *et al* 1973), which has been used in investigations of fields and forces generated by castellated electrodes (Wang *et al* 1993) and travelling-wave electrode arrays (Hughes *et al* 1996). This numerical system has been shown to determine electric field distributions to a high degree of accuracy when compared to both the precise analytical solution (Wang *et al* 1996) and other field solvers (Hughes *et al* 1995) in moving-field simulations of this kind. Comparisons between simulation of electric fields in polynomial electrodes performed both by this model and the commercial finite-element software Maxwell (Ansoft ltd) indicate a high degree of conformity both in terms of field morphology and absolute values.

The electrode model replicates the most common form of electrorotation array, *viz*. an arrangement of four identical electrodes placed symmetrically about a central axis, to

which sinusoidal signals are applied in quadrature (as shown in figure 1). Electrodes were simulated as being 200nm thick, in keeping with typical values for electrodes fabricated by lithographic techniques. For further descriptions of the model used in this work, refer to Hughes *et al* (1994).

For the purposes of this work, the spacing between opposing electrode tips was fixed at 400μm. This is a typical size for electrodes used in the study of cells, remained constant between the various electrode geometries presented here. As many cells (e.g. yeast cells, erythrocytes) are approximately 6μm in diameter, the simulation was performed in the plane 3μm above the upper surfaces of the electrodes which coincides with the centre of such cells. The solution was examined across the square defined by the electrode tips (illustrated by the boxed region in figure 1) which was divided into a regular matrix of 40x40 points.

Previous work (Hughes *et al* 1994) has shown that the electric field $\vec{E}$ acting in the region between the electrodes is of the form:

$$\vec{E} = \vec{E}_x \cos(\omega t + \varphi_x)\vec{a}_x + \vec{E}_y \cos(\omega t + \varphi_y)\vec{a}_y \qquad (1)$$

where $\vec{a}_x$ and $\vec{a}_y$ are the unit vectors in the x- and y- directions. The dynamic rotating electric field was simulated by dividing the rotation cycle into 36 10º "frames" and determining the *static* electric field distribution in these instances. A sinusoidal signal of peak amplitude 10 x sin(10°x fnumber) Volts, where fnumber is the frame number in the cycle, was applied to the first electrode. The potential on each successive electrode

was phase-shifted by a further multiple of 90° to produce quadrature as shown in figure 1.

Calculations were performed using FORTRAN 77 on a VAX computer, and the results were processed using MATLAB (The Math Works) to determine the spatial variation of the magnitude (E_X, E_Y, E_Z) and phase (φ_X, φ_Y, φ_Z) of the rotating field. Previous work (Hughes *et al* 1994) has shown that the time-averaged torque Γ in the inter-electrode chamber is given by equation 2.

$$\vec{\Gamma} = -4\pi\varepsilon_m r^3 \operatorname{Im}(f_{CM}) E_x E_y \sin(\varphi_x - \varphi_y)\vec{a}_x \times \vec{a}_y . \qquad (2)$$

It is possible to derive from equations (1) and (2) a factor which describes the uniformity of the rotational torque exerted on the particle as a function of its location. We define this field factor E_{eff}^2 as follows:

$$E_{eff}^2 = E_x E_y \sin(\varphi_x - \varphi_y). \qquad (3)$$

The variation of E_{eff}^2 across the electrode chamber indicates that the induced torque is not generally proportional to the square of the field strength. Studies (Hughes *et al* 1994) have shown that E_{eff}^2 varies across the electrode chamber more widely than had previously been predicted, a fact which has considerable bearing on electrorotation spectra taken for particles at different points within the chamber. An example of the variation of E_{eff}^2 as a function of position within an electrode chamber of the "polynomial" geometry is given in figure 2.

3. Results and Discussion

The common practice when performing rotation experiments is to place a number of particles in the electrode chamber and observe their motion using a microscope and video camera. The rotation rate of the particles is determined by measuring the time taken to perform one revolution. For statistical purposes it is advantageous to perform analysis on a number of cells simultaneously, and experiments are often videotaped to allow measurements to be taken in "parallel" later. Since the particles occupy many positions across the chamber, and the magnitude of induced torque varies across the electrode chamber, it would be wise to introduce some method of compensation in order for particle rotation rates to be comparable.

It has been suggested (Hughes *et al* 1994) that a correction factor based on the normalised E_{eff}^2 distribution may be superimposed across an electrode chamber in experimentation for use in automated electrorotation (De Gasperis *et al* (1998), Zhou *et al* (1998)). Such a system could incorporate a location-variable correction coefficient into the automated rotation rate measurement software, which could adjust the recorded rotation rate according to particle location within the chamber. However, for direct observation using a microscope and stopwatch, such a system is obviously impractical.

In place of the rotation correction system, a more viable alternative is to employ masking, whereby only a section of the rotation chamber in which the torque is known to be relatively constant is studied, whilst the remainder of the electrode chamber is "masked off" and not studied. As a consequence the measured rotation rates are

directly comparable. This method requires considerably less effort than would be needed to implement position-determined adjustment factors.

Finally, since ROT requires the use of large electric field strengths, it is a necessary but unwelcome side-effect that, near the electrode edges, translational motion induced by dielectrophoresis (DEP) is observed. This serves to move cells within the chamber (typically towards, or away from, the electrode edges) which in turn causes the rotation rate to change or to cause the cell to stick to the electrode edge, thereby becoming unusable for ROT measurements. Therefore we must consider the effects of DEP force when considering the optimum conditions for ROT.

3.1 Polynomial Electrodes

There are two principal means by which AC electrokinetic effects introduce errors in the determination of electrorotation rate; the variation in torque across the electrode chamber, and the translational (Dielectrophoretic) force causing studied particles to drift across the chamber during the experiment. These factors may be simulated, and figure 3 shows them for a polynomial-type electrode structure.

As can be seen from figure 3(a), the variation in E_{eff}^2 is small at the centre of the chamber, but increases markedly towards the electrode tips. Within the region most often used by those involved in electrorotation experiments, variation in E_{eff}^2 increases to above 20% of that at the centre outwith a region approximately defined by a box with edges halfway between the centre and electrode tips. Variation in excess of 50% is seen at the electrode edges (at the centre of the edges in Figure 3(a)), which is in practice compounded by a strong *z*-component rotation. The simulation results also indicate that

the rotation rate drops dramatically towards the corners of the area, between adjacent electrodes, shown as the contours seen in the *corners* of 3(a). In the centre of the electrode chamber the particles are almost planar to the electrodes, and the effect of the *z*-component of both electrorotational torque and dielectrophoretic force is negligible (Hughes *et al* 1994).

Figure 3(b) shows the normalised DEP force acting towards the electrode edges. This is very low in a region at the centre of the electrodes, and rises sharply beyond the region approximately defined by the same box described above; particles near to the electrodes may drift towards (or away from) the electrodes under the influence of dielectrophoresis. Over extended periods (such as determination of time-variant properties of cells where experiments may continue for up to a day or more) this becomes significantly more important.

It would therefore be reasonable to say that for geometries of planar polynomial design, it is preferable to restrict experiments only to those particles within a square with edges half-way between the chamber centre and the electrode tips. Within that box, E_{eff}^2 varies by approximately 20% according to its position, as described in figure 3(a). This correlates well with experimental work (Hughes, Archer and Morgan, in preparation) where, within this box, the rotation rate of elliptical beads was found to vary by 15-20% of the centre value at the edges of the box.

3.2 Effect of electrode geometry

Using the methods of analysis described above, it is possible to compare different electrode designs in a quantitative manner by considering both the magnitude of torque

produced, and the degree of variation in that torque across the boxed region described above. Previous studies of this nature (Gimsa 1988; Hölzel 1993) have only compared the RMS electric field distribution without accounting for phase variation; the studies presented here also consider phase effects in determining torque distribution.

The ideal electrode geometry for ROT measurements would induce a uniform torque across a large area of the electrode chamber. Induced torque should be as large as possible, so that the rate of particle rotation is not overly influenced by factors such as Brownian motion and fluid flow. By combining these two basic criteria, a quality factor Q for the evaluation and comparison of different geometries may be defined as

$$Q = A\,\Gamma_C \qquad (4)$$

where Γ_C is the torque at the centre of the electrode chamber, and A is the percentage of continuous area of the electrode chamber where the torque does not vary from Γ_C by more than an arbitrary amount. In most cases the outer limits of our region of interest, defined by the boxed region described previously, delineate the area of approximately 20% torque variation (i.e. $\Gamma = 1.2*\Gamma_c$); we can quantify the rate of variation of torque within this region by determining the size of the region enclosed by the 5% ($1.05*\Gamma_c$) and 10% ($1.1*\Gamma_c$) boundaries.

The ten different electrode geometries studied are as shown in figure 4. Many of these geometries have been employed in practical experiments by other researchers (e.g. Arnold and Zimmerman 1982; Burt *et al* 1995 ; Huang and Pethig 1991; Hölzel 1993; Gimsa *et al* 1988; Fuhr *et al* 1984), whilst others are arbitrary shapes which were

included for comparison with existing designs. The designs used were as follows: polynomial, bone (a polynomial with a concave tip), pointed and truncated pyramidal, square (wide electrodes stretching the length of the chamber), pin, and a range of elliptical patterns with axes in the range 2:3 (oblate), 1:1 (circular), 3:2 (prolate) and 2:1 (also prolate).

The results of these simulations are presented in table 1, where values of Q are calculated for values of torque within 5% and 10% variation from Γ_C. Notably, all the electrode geometries save the pin geometry have a region of highly similar size and shape within which the torque remains within 5% of Γ_C. However, where a 10% boundary is considered there is a variation between different geometries of nearly x2 between the best and worst cases. There is also a wide variation in values of Γ_C, with an order of magnitude separating the largest and smallest values. Generally, the configurations with the higher electric fields, and hence greater values of Γ_C, also generate widely non-uniform fields and thus the lower values of A. The geometries with the greatest values of Q are those which balance these two factors, with values of A and Γ_C which are both above average but not markedly so.

These simulations indicate that the electrode geometries that produce the greatest values of Q are the polynomial (Huang and Pethig 1991) and bone (Burt et al 1995) electrodes, both of which have been employed in practical experimentation. In general, we observe the trend that geometries where the sides of neighbouring electrodes were approximately parallel, such as the polynomial and bone type, plus the pointed and truncated pyramid geometries which were designed for this simulation, generate more uniform electric fields. Electrode structures where the sides of neighbouring electrodes

are close to one another, such as the square and polynomial geometries, generate higher electric fields and thus greater values of torque. It is the combination of both these factors, where electrodes are approximately parallel but approach each other at a relatively large distance from the electrorotation chamber itself, that gives geometries such as the bone and polynomial types their superior performance. It should also be noted that the square geometry, whilst not quite achieving the general performance of the polynomial and bone geometries at 10% variation, has far superior performance at the 5% margin. This design is amongst the easiest to fabricate of the geometries described as it does not feature complex curved edges. Therefore we include this design amongst those recommended for general electrorotation measurements. In contrast to these the pin geometry (Arnold and Zimmermann 1982), often employed in experimentation due to its ease of construction, has a particularly poor value of Q owing to its small, non-uniform electric field. This would imply that it is less suitable for ROT experimentation than the other geometries discussed here.

4. Conclusion

As the technique of Electrorotation begins to make the transition from the laboratory towards general practical use, it becomes increasingly important to find methods of improving the accuracy of experimental data whilst minimising the complexity of the measurement system. To this end we have presented an examination of the distribution of torque across the electrode chamber. In this manner, we have shown that the optimal region for performing ROT experiments is defined by the square covering the inner 25% of the electrode chamber, within which the torque varies by approximately 20%. Furthermore, by comparing both the magnitude and variation of the torque generated in this region, the most appropriate electrode design for a given application may be found. This study indicates that electrodes with wide, inward-facing planes give the highest torque, those of a triangular design give the largest areas of uniform torque, and that polynomial or saddle-shaped electrodes offer the most practical compromise between these two factors.

Acknowledgements

Much of the simulation work presented in this paper was performed at the University of Wales at Bangor, UK. The author would like to thank Prof. Ron Pethig and Drs Xiao-Bo Wang, Ying Huang, Julian Burt and Ka Lok Chan for their assistance and valuable discussions.

References

Archer S, Morgan H and Rixon FJ 1997 Electrorotational studies of Baby Hamster Kidney fibroblasts (C-13) following infection with Herpes Simplex Virus, type 1 *Biophys. J*. **72** Tu-pos 381

Arnold W M and Zimmermann U 1982 Rotating-field-induced rotation and measurement of the membrane capacitance of single mesophyll cells *Z. Naturforsch*. **37c** 908-915

Birtles A B, Mayo B J and Bennett A W 1973 Computer technique for solving 3-dimensional electron-optics and capacitance problems *Proc. IEE* **120** 213-220

Burt JPH, Pethig R, Hughes MP, Kerslake JP, Parton A and Dawson D 1995 Electrorotation assay (ERA) for cryptosporidium and giardia from raw water supplies *Proc. 9th Int Conference on Electrostatics*

Chan KL, Gascoyne PRC, Becker FF and Pethig R 1997 Electrorotation of liposomes; verification of dielectric multi-shell model for cells *Biochim. Biophys. Acta* **1349** 182-196

De Gasperis G, Wang X-B, Yang J, Becker FF and Gascoyne PRC 1998 Automated electrorotation: dielectric characterization of living cells by real time motion estimation *Meas. Sci. Technol*. (in press)

Fuhr G, Hagedorn R and Göring H 1984 Cell rotation in a discontinuous field of a 4-electrode chamber *Studia Biophysica* **102** 221-227

Gimsa J, Glaser R and Fuhr G 1988 Remarks on the field distribution in four electrode chambers for electrorotational measurements *Studia Biophysica* **125** 71-76

Hölzel R and Lamprecht I 1992 Dielectric propertis of yeast cells as determined by electrorotation *Biochim. Biophys. Acta* **1104** 195-200

Hölzel R 1993 Electric field calculation for electro-rotation electrodes *J. Phys. D: Appl. Phys* **26** 2112-2116

Hölzel R 1997 Electrorotation of single yeast cells at frequencies between 100Hz and 1.6GHz *Biophys. J.* **73** 1103-1109

Huang Y, Hölzel R, Pethig, R and Wang X-B 1992 Differences in the AC electrodynamics of viable and non-viable yeast cells determined through combined dielectrophoresis and electrorotation studies *Phys. Med. Biol*. **37** 1499-1517

Huang Y and Pethig R 1991 Electrode design for negative dielectrophoresis applications *Meas. Sci. Technol*. **2** 1142-1146

Hughes MP, Wang X-B, Becker FF, Gascoyne PRC and Pethig R 1994 Computer-aided analyses of electric fields used in electrorotation studies *J. Phys. D: Appl. Phys* **27** 1564-1570

Hughes MP 1995 Electrokinetic Manipulation of Particles: Computer-Aided Studies *PhD thesis; University of Wales, Bangor UK*

Hughes MP, Pethig R and Wang X-B 1996 Forces on particles in travelling electric fields: computer-aided simulations *J. Phys. D: Appl. Phys* **29** 474-482

Wang X-B, Huang Y, Burt J P H, Markx G H and Pethig R Selective dielectrophoretic confinement of bioparticles in potential-energy wells 1993 *J. Phys. D: Appl. Phys* **26** 1278-1285

Wang X, Wang X-B, Becker FF and Gascoyne PRC 1996 A theoretical method of electrical field analysis for dielectrophoretic electrode arrays using Green's theorem *J. Phys. D: Appl. Phys.* **29** 1649-1660

Zhou X-F, Markx GH, Pethig R and Eastwood IM 1995 Differentiation of viable and non-viable bacterial biofilms using electrorotation *Biochim. Biophys. Acta* **1245** 83-93

Zhou X-F, Burt JPH and Pethig R 1998 Automatic cell electrorotation measurements: studies of the biological effects of low-frequency electromagnetic fields and of heat shock *Phys. Med. Biol*. (in press)

Figure Legends

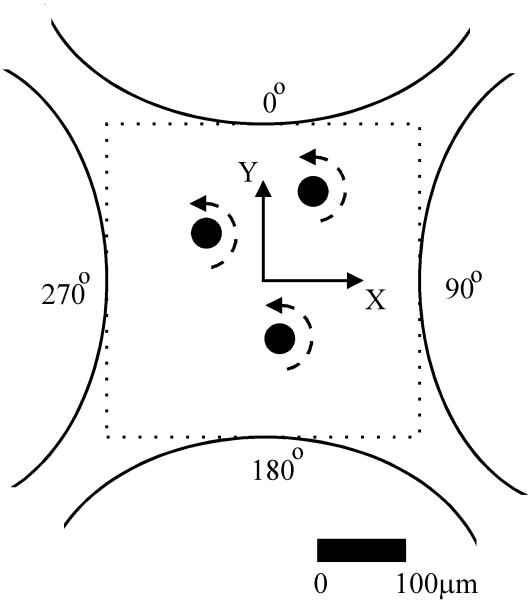

1 Schematic of a polynomial electrode array, as used for Electrorotation (ROT). Particles are suspended within a rotating electric field generated by four electrodes in quadrature. The square region denotes the area analysed in this study.

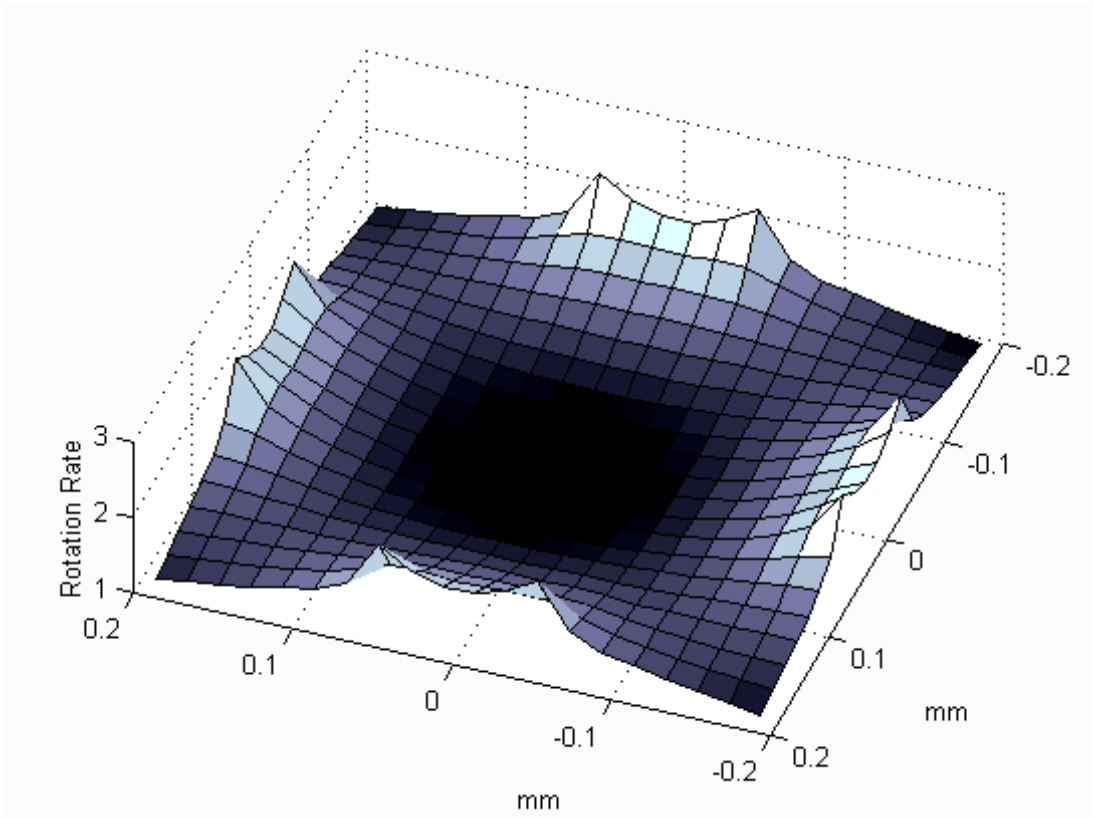

2 Spatial variation of the field factor E^2_{eff} ($V^2\mu m^{-2}$) across the region defined in Figure 1, as generated by a polynomial electrode array. Note the degree of variation in field factor (and consequently induced torque) between the centre and edge of the array.

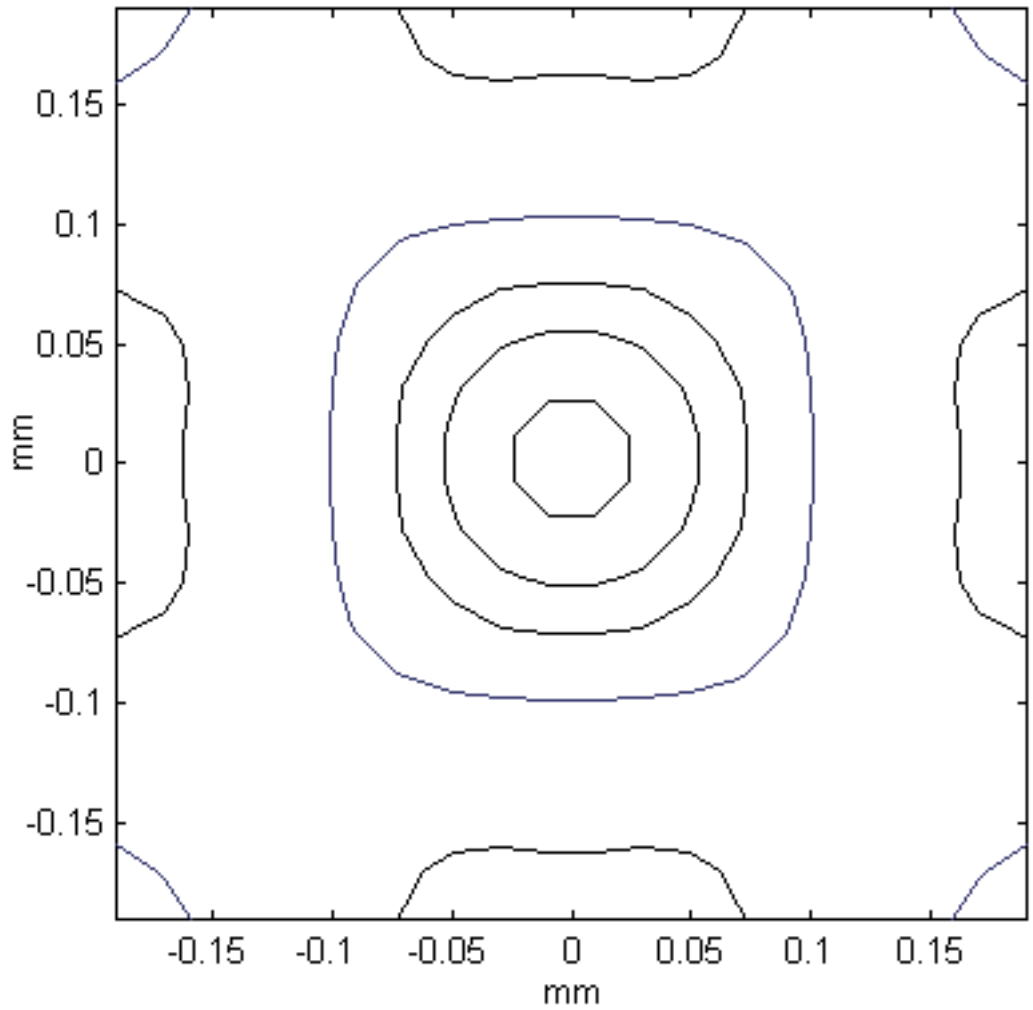

3(a) Variation in torque from the value at the centre of electrode chamber. Lines indicate (from centre) the limits of 1%, 5%, 10% and 20% variation. Variation in excess of 50% is visible near electrode tips (at the centre of each edge). A sharp decline in rotational torque towards the corners of the box visible in the corners of the box, where the torque drops *below* 20%.

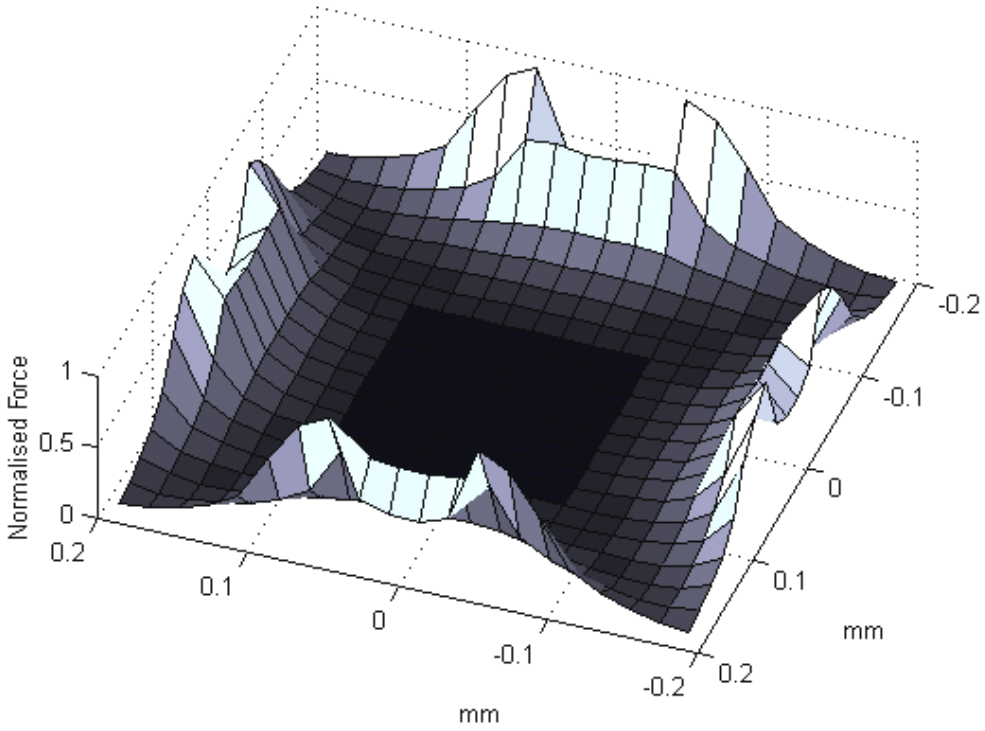

3(b) Normalised dielectrophoretic force across the region defined by the electrode tips, and 3μm above the electrode plane.

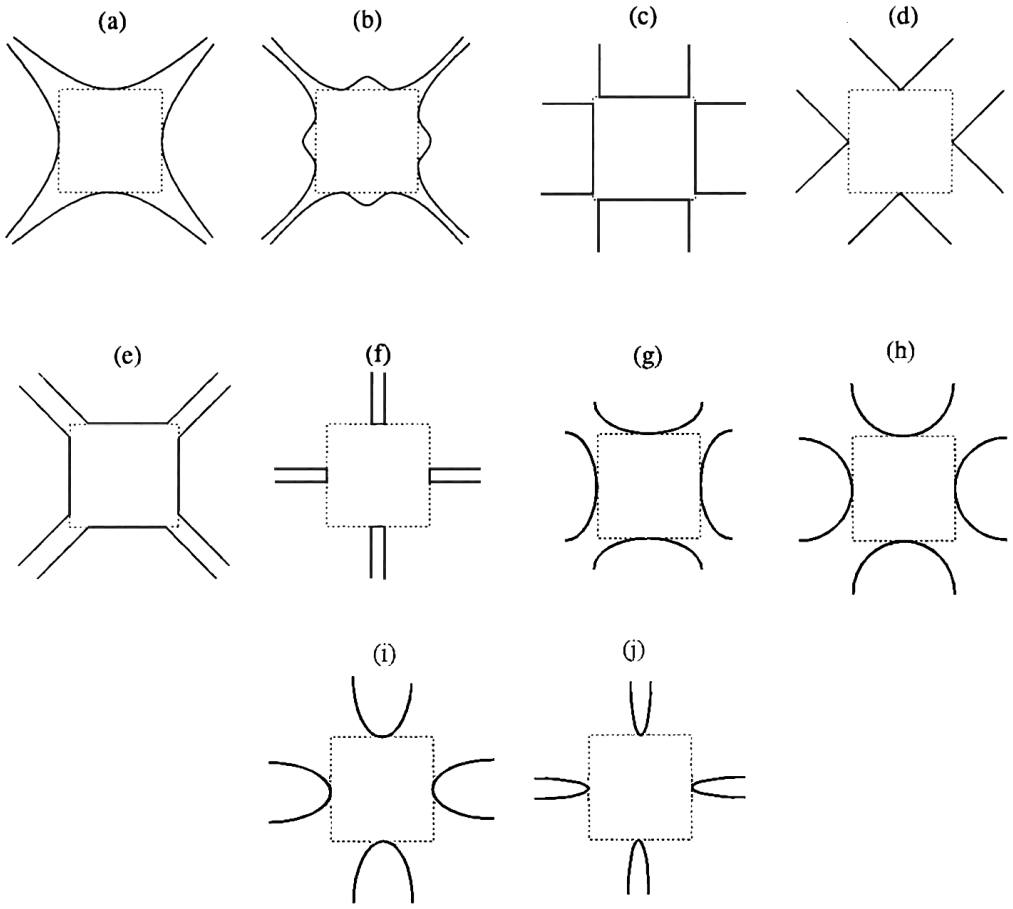

4 Schematics of the electrode designs studied here. (A) polynomial (b) bone (c) square (d) pointed pyramidal (e) truncated pyramidal (f) pin (g) oblate ellipse (h) circular (i) prolate ellipse, (j) narrow prolate ellipse.

Table Legends

1 A comparison of the suitability of various electrode geometries for electrorotation studies. Analysis is presented in terms of torque at the centre of the array Γ_c ,percent area A within which the torque does not deviate from Γ_c by an arbitrary limit (either 5% or 10%), and quality factor Q as described in the text. Index letter refer to illustrations in figure 4

Electrode Shape	**Effective Torque at Centre Γ_C , x10^{-4}**	**5% Deviation from Γ_C**		**10% Deviation from Γ_C**	
		A(%)	**Q, x10^{-3}**	**A(%)**	**Q, x10^{-3}**
a. Polynomial	4.56	6	2.74	13	5.93
b. Bone	4.49	6	2.69	13	5.84
c. Square	5.28	6	3.7	11	5.81
d. Pointed Pyramidal	2.69	6	1.61	15	4.04
e. Truncated Pyramidal	4.79	6	2.87	11	5.27
f. Pin	0.53	4	0.21	8	0.42
Ellipses:					
g. 2:1	1.97	6	1.18	9	1.77
h. 3:2	2.38	6	1.43	9	2.14
i. 1:1	4.00	6	2.40	11	4.40
j. 2:3	4.91	6	2.95	11	5.40